International Journal for Research in Engineering Application & Management (IJREAM)
ISSN : 2454-9150 Vol-08, Issue-09, Dec 2022

Assessment of Land Surface Temperature of Mining Area in Part of Karimnagar and Adilabad Districts, Telangana Using Satellite Data

Nagaraju Thummala[1], A. Narsing rao[2], Rajendra Prasad Kanchi[3]

1: Geology Dept, Osmania University, Hyderabad, Telangana, India, tnr.2020@gmail.com

2, 3: Professors, Geology Dept, Osmania University, Hyderabad, Telangana, India, narsing1958@gmail.com, rpcanchi05@osmania.ac.in.

Abstract: In Mining studies, energy input to the Mining variation is an important component. Generally, ground measured temperature used as an alternative indicator of energy input. Recently, developing spectral reflectance with Temperature from satellite data have revealed a wide range of statistical Technical applications in Land use/Land cover (LULC) classification can combine both advantages, which is beneficial for accurate feature. Identification of Land degradations due to mining using Remote Sensing Statistical Techniques (RSST) is one of the most important challenges of nature conservation. In this research, Land Surface Temperature (LST) are economical, suitable and performed from AASTER and LANDSAT-8 satellite simultaneously with ground reference data selected some Mandal wise area around the Godavari basin (Old Karimnagar and Adilabad) study area background polygons. Linear Regression Analysis (LRA) was performed in iterative mode based on Thermal bands acquired from AASTER and LANDSAT-8 with field air Temperature. The deviation between the LST obtained from AASTER data and field air temperature is generally within +/- 4^o. The deviation between the LST obtained from LANDSAT-8 data and field air temperature is generally within +/- 5^o. The deviation between LST derived from AASTER data and that of LANDSAT-8 data is generally within +/- 4^o. The estimated LST values and Field air temperature have a general difference of about 4^o. In view of the above cited reasons the deviations may still be acceptable. However, the factors such as, time of satellite overpass, possible inaccuracies in exact locations of field stations and coarse spatial resolution of satellite data are responsible for some deviations in the actual measured and estimated temperatures. This experiment with larger data set and some more field stations can improve the accuracy of estimation.

Key points: Satellite data, Land Surface Temperature (LST), Mining Surface Temperature (MST), Field Air Temperature. Atmospheric correction, Reflectance and radiation, spectral radiance, surface reflectance, spectral brightness Temperature

I. INTRODUCTION

Land Degradation due to mining could be defined as a loss of carbon stocks from forestland and agriculture with land cover change caused by either natural or anthropogenic activities with relating to climate change [1, 2]. Land degradation, Deforestation due to mining has become an important issue concerning climate change, and has been the second leading cause of anthropogenic greenhouse emissions. Mining area surrounded by some deferent features occupied such as built-up area, bare soil, agriculture, and forest and water bodies. Minimum mining area covered from agriculture surrounding area and maximum covered in forest. Thus there is a gradual increase in mining cover area from year to year. Normally, mining maximum should be surrounding the Godavari basin [11, 12]. Mining area is reflecting more compare to other non mining area. Deferent material reflecting deferent type spectral values based on earth features. The reflect values is interlink with temperature. Land Surface Temperature (LST) is an important parameter for many scientific disciplines since it affects the interaction between the land and the atmosphere [3, 14]. Many LST retrieval algorithms based on remotely sensed images have been introduced so far, where the Land Surface Emissivity (LSE) is one of the main factors affecting the accuracy of the LST estimation [4, 14]. In addition to mining cover area [5], the Mining Surface Temperature (MST) is important to address the energy input to the degradation

 DOI : 10.35291/2454-9150.2022.0489

area for due to mining [10], built-up, bare soil area [4,5]. Atmospheric correction is a necessary step in processing data recorded by space borne sensors for cloudless atmosphere [6], primarily in the visible, near-IR spectral and SWIR range [7]. Many methods based on radioactive-transfer models and empirical approaches with prior knowledge have been developed for the retrieval of Hyperspectral and Multispectral surface reflectance [8, 9]. Satellite images provide a complete spectrum for every pixel over the wavelength range from 0.4 to 2.5m [8, 9], and the at-sensor radiance images contain absorption and scattering by atmospheric gases and aerosols. Atmospheric correction is a process in order to remove the atmospheric effects and retrieve the surface reflectance for further applications [2], such as land cover classification [3]. A sample compares at-sensor radiance spectrum and the corrected reflectance spectrum from a typical Hyperspectral and multi spectral sensors [9, 8]. The air temperatures were measured in the field at a few stations within the Godavari basin (Old Karimnagar and Adilabad Dist).The temperature measured at these limited stations does not completely explain the horizontal and vertical spatial variability within the basin. It is therefore being experimented; to estimate the Land Surface Temperature (LST) using Thermal Band Satellite Data (TBSD) [14] and compare with field measured Air Temperatures (AT) so that the technique can be used operationally in the ongoing project. In the present studies main analytical parts are 1) Digital number to radiance and radiance to reflectance 2) using the reflectance values identified Land Surface Temperature (LST) for spectral band values verification 3) Regression analysis between Thermal bands from AASTER and LANDSAT-8 satellite data with field air Temperature from selected small area 4) Statistical analysis applied to all over study area and get Mining Land surface Temperature data.

II. Study Area and Data Used

The study area is depicted in fig-1. Godavari basin area Around Old Adilabad and Karimnagar district lies between 77^{0} $37^{!}$ $20.16^{!!}$ to 80^{0} $19^{!}$ $53.22^{!!}$of the eastern longitudes and 17^{0} $58^{!}$ $55.67^{!!}$ to 19^{0} $55^{!}$ $27.88^{!!}$ of northern latitudes. The districts is bounded on North by Maharashtra state boundary, on the East by Warangal districts of Telangana and on the South by Siddipet on the West by Nizamabad Dist of Telangana and Nanded district of Maharashtra State. Godavari River is dividing the two districts [12]. These harbor mainly dry deciduous forest and aborigines. These forests occupy about 34.5 percent of the total geographical area of the districts. Godavari river basin in south India is the study area. The river Godavari is India second largest basin in India of the main tributaries of as its origin near Trimbakeswara, Nasik at Maharashtra an elevation of about 920m (approx.) [10, 12].Characteristics of the basin and inaccessibility of the major part of it make remote sensing application ideal for geologists to monitor the Radiance information of the region and assess the resulting Mining resource [13].

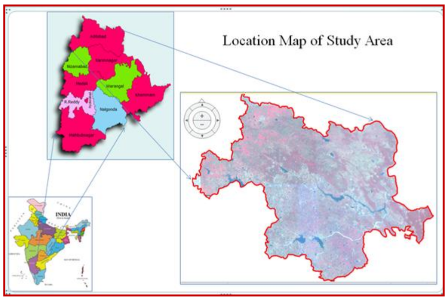

Fig.4.1: Location map of the study area (Godavari basin: Old Karimnagar & Adilabad dist)

The gross cropped area during 2019-20 is 1,56,693 ha. Forest occupies 32% of the total geographical area, waste lands occupies 9% of area. Paddy is main crop with 36% sown area

Under Exploratory drilling CGWB hs drilled 28 wells, 02 well of shallow depth of 30 m, 05 wells of 30-100 m depth, 04 wells of 100-200m depth and 17 wells of 200-300 m depth**.** 10 representative exploratory well data of SCCL also utilized for the conceptualization of the Aquifer system in the area Geophysical data from 30 VES data (CGWB) [12] reveals resistivity of different formations depth wise [11].

III. Methodology

In this Research methodology main steps have 1) DN to Radiance and Radiance to Reflectance from satellite data, 2) Radiance to Land surface Temperature (LST) 3) Compare satellite LST with Field surface Temperature using statistical analysis 4) Identification of coefficient, Constant and Slope values using \Linear Regression equation in between air temperature and multispectral satellite data [14]. The land surface reflectance values of mining area was different values compared to the other none mining area. Deferent material reflecting deferent type spectral values based on earth features [8, 9]. The Land Surface Reflectance (LSR) values is interlink with Land Surface Temperature (LST) [14]. Land Surface Temperature (LST) is an important parameter for many scientific disciplines since it affects the interaction between the land and the atmosphere. Many LST retrieval algorithms based on remotely sensed images have been introduced so far, where the Land Surface Reflectance(LSR) [14] and Land Surface Emissivity (LSE) is one of the main factors affecting the accuracy of the land degradations due to mining estimation[14, 10]. In addition to mining cover area, the mining surface temperature is

 DOI : 10.35291/2454-9150.2022.0489

important to address the Land Surface Reflectance (LSR) (energy) input to the mining area for due to degradation area [10], mining, built-up, bare soil area [15]. So Land Surface Temperatures (LST) was measured in the study area at a few stations within the Godavari basin [14] (Old Karimnagar and Adilabad [14, 10]. It is therefore being experimented, to estimate the Land Surface Temperature (LST) using thermal bands from LANDSAT-8 and AASTER satellite data compare with The aim was to establish ground reference polygons covering the nine pixels (3× 3) in each area such as Mining area and none mining area [16] (built up area, bare soil area, Agriculture, forest and water bodies). The polygons were only used to indicate the coordinates of each classified field area from LANDSAT-8 and AASTER satellite data [16, 14]. The areas thus determined were then used to identify Maximum to minimum spectral temperature from the data in each classified area [14].

A statistical analysis (Linier Regression) was carried out between the LST derived from AASTER [16]& LANDSAT-8 LST maps and Land Surface Temperature(LST) measured in the field [14], where as downloaded from 'Open Data Telangana' (ODT) from the website browser is http://data.telangana.govt.in/dataset/telangana- temperature-data-2022/resource in to determine the relationship and mutual comparison for verification of Land surface Reflectance (LSR) [17].

The Land surface Temperature (LST) data measured at approximately Mandal wise from entire old Karimnagar and Adhilabad district have been used in this study [14, 17]. In this research, a sufficiently accurate method of Top of atmospheric correction used based on the analytical solutions of radioactive equation used [6]. The analytical solution equations can be used to calculate the accuracy Land Surface spectrum of outgoing radiation at the top boundary of the cloudless atmosphere (water droplet dust, ice crystals). The analytical solution of the Land Surface Reflectance (LSR) [6] for finding unknown parameters of the degraded area was carried out by the method of radiation analysis for an individual selected digital pixel value of the image, taking into account the adjacency effects [14,16]. Using the parameters of the atmosphere and the average Land surface reflectance(LSR), and also assuming homogeneity of the atmosphere within a certain study area selected from the LANDSAT-8 and AASTER satellite image [16,18](or within the whole Image), the accuracy spectral reflectance values at the Earth's surface was calculated for all over study area[14]. A comparison with the results of atmospheric correction with Land Surface Temperature (LST) data which was analyzed by AASTER, LANDSAT-8 data has been performed. Finally [16, 18], to valuable data obtained by this method, a comparative analysis with satellite data based measurements of the Radiometric Calibration Network (RadCalNet) was carried out

4.3. Data Browse

The AASTER image LST products are in degree Kelvin (ºK) [16] as 12 bit continuous data with scale factor of AASTER is 0.01 in projection parameters1 projection. The AASTER temperature data products were re-projected from LANDSAT-8 data projection/WGS84 datum to Lambert conformal conic and WGS84 datum, [16, 18] Zone-44_E using the rigorous transformation in ERDAS Imagine. The re-sampling was done using Nearest Neighbor method, which uses the value of the nearest pixel to assign to the output pixel value [14]. Then the re-project image is subset with the Godavari basin boundary so as to obtain the area of interest. However, it was observed that all AASTER data products were found to be very accurately geo referenced. In order to find out AASTER data were available, search the AASTER archives at the EROS Data Center's Land Processes DAAC through the EDG [19]. All acquired and processed ASTER data are archived and distributed from here (http://edcimswww.cr.usgs.gov/pub/imswelcome/) [16, 19]. The AASTER Level-1B data are offered in terms of scaled radiance the ground surface temperature downloaded from 'Open Data Telangana' (ODT) from the website browser is http://data.telangana.govt.in/dataset/telangana-temperature-data-2022/resourcein [17]. The temperature was downloaded in EXL format from Mandal wise in karimnagar and Adilabad, Telangana from January to May month, 2022. These data values contain maximum and minimum temperatures in Exl format. The max and min temperature data converted to average temperature data to each location.

Top of Atmosphere corrections: 1) Digital number to Radiance:

The Land Surface Temperature was the temperature of a mine body that would emit an identical amount of radiation at a definite wavelength (um) [3, 14] and it can be calculated by the Planck function. Considered, LANDSAT-8, AASTER satellite bands (Thermal Infrared (TIR pixel values) was firstly converted into radiance from Digital Number (DN) values. Radiances for Spectral band of Landsat-8, AASTER satellite data were obtained using Equation (4.1) [1, 16]. Radiance to surface reflectance values of spectral bands of these satellite data can be retrieved from Equation (4.1)

$$L_\lambda = \frac{(L_{MAX-} - L_{MIN})}{Q_{CALMAX} - Q_{CALMIN})})] \times [Q_{CAL} - Q_{CALMIN}] + L_{MIN} \quad \text{------------} (4.1)$$

 DOI : 10.35291/2454-9150.2022.0489

where L_λ is Top of Atmosphere (TOA) spectral radiance (Watts/(m^2.srad.µm), Q_{CAL} is the quantized calibrated pixel value in DN, $L_{MIN\_}$ (Watts/(m^2.srad.µm)) is the spectral radiance scaled to Q_{CALMIN}, $L_{MAX\_}$ (Watts/(m^2.srad.µm)) is the spectral radiance scaled to Q_{CALMAX}, Q_{CALMIN} is the minimum quantized calibrated pixel value in DN and Q_{CALMAX} is the maximum quantized calibrated pixel value in DN. $L_{MIN\_}$, $L_{MAX\_}$, Q_{CALMIN}, and Q_{CALMAX} were All of these variables can be retrieved from the metadata file of LANDSAT-8 and AASTER data [16,18]. After conversion of radiance pixel values of land surface converted to Land Surface Temperature (LST) image can be generated from LANDSAT-8 and AASTER satellite data images [1, 2, 16].

2) Radiance to Reflectance

The Digital to Radiance and Radiance to surface reflectance calculation steps for Modified Simple Ratio Difference Mining Index (MSRDMI) from LANDSAT-8 satellite data were described. For the MSRDMI data firstly[20], Digital to radiance conversion was applied as in Model Maker in Erdas Imagine and then Radiance to reflectance value can be calculated by radiances using equation (4.2) [1,16]. For Landsat-8, AASTER satellite data, reflectance conversion can be applied to DN values directly as in Model Maker in Erdas Imagine [2, 14].

$$\rho = \frac{\pi L_\lambda d^2}{E_{SUN} cos\theta} \text{ --------------- (4.2)}$$

Where ρ is unit less reflectance, L_λ is the TOA spectral radiance (Watts/(m^2.srad.µm)), d is Earth-Sun distance in astronomical units, $E_{SUN\lambda}$ is the mean solar exo-atmospheric spectral irradiances (Watts/(m^2·µm)) and θ is the solar zenith angle in degrees. E_{SUN} values for each bands of Landsat-8, AASTER and can be obtained from the metadata (handbooks) of the related mission [1, 16]. θ & d values can be attained from the metadata file.

Land Surface Temperature (LST)

Temperature is a linear relationship between the Radiance (Reflectance) and Temperature in the two far infrared windows. Since the two thermal bands of AASTER and LANSAT-8 are close enough to each other but still have different transmittance and emissivity [16, 18], an equation system describing the thermal radiance reaching the Remote Sensor in the two bands can be established, which consequently enables the solution of LST. This makes the estimation of LST from the two thermal bands of AASTER and LANSAT-8 data [16, 18. The derivation of LST retrieval is based on the Thermal Radiance of the ground and its transfer from the ground through the atmosphere to the Remote Sensor [23]. Generally speaking, the ground is not a blackbody. Thus ground emissivity has to be considered for computing the Thermal Radiance emitted by the ground. Atmosphere has important effects on the received radiance at Remote Sensor level [22]. The extensive need of land surface temperature (LST) for study of the Earth's environment and resources has made the retrieval of LST from Remote Sensing data an important topic in the last three decades [21]. Before extracting Land Surface Temperatures (LST) from Thermal bands, the images were geometrically and radio metrically corrected. Next step was to convert spectral radiance to radiant (black body) Temperature [14]. This procedure requires implementing Planck's law, which describes emissivity of a black body depending on wavelength and absolute Temperature. Then the radiant temperature was recalculated to Land Surface (kinetic) Temperature including atmosphere influence and emissivity correction [6].

Land Surface Temperature Using LANDSAT-8

Radiometric calibration is required for Landsat 8 OLI data, the digital number can be converted to apparent reflectance using the reflectance rescaling factor coefficients in the header file [18]. To conduct cloud detection experiments using Landsat 8 data with surface reflectance product support. The spectral differences between the two sensors must be considered for estimating Land Surface Temperature (LST) from LANDSAT-8 satellite, (18) after conversion of Digital pixel values to Radiance as per discussed in top of atmosphere chapter [6, 18]. Thermal Infrared Sensor (TIR) to determine LST and MST values in model maker algorithm [14, 16, and 18]. This algorithm requires as input values of surface emissivity region that 10 and 11 bands (Table4.1) from operating in 10.6-11.19µm and 11.5-12.51µm, K_1 and K_2 respectively for surface temperature monitoring. Remote sensing of LST can be formulated as follows equation A.3. [16] The K_1 and K_2 values evaluated from as shown in the tableB1

$$T = \frac{K2}{\ln(\frac{K1}{L}+1)} \text{ \_\_\_\_\_\_\_\_\_\_ (4.3)}$$

 DOI : 10.35291/2454-9150.2022.0489

Where T refers to the effective at-satellite temperature in Kelvin, K1 (Watts/(m^2.srad.µm)) and K2 (Kelvin) are the calibration constants and L_ is the spectral radiance. The values of the constants (K1 and K2) were presented in Table 4.2 since they change from sensor to sensor [1, 2]

***Table4.1.** Landsat thermal bands specifications.*

Sensor	Wavelength	Resolution	Band
LANDSAT-5	10.40-12.50	120	B6
NANDSAT-7	10.40-12.50	60	B6
LANDSAT-8	10.60-11.19	100	B10
LANDSAT-8	11.50-12.51	100	B11

***Table4.2:** Thermal band calibration constants for Landsat satellites.*

SATELLITE	K1 (Watts/(m2_srad__m))	K2 (Kelvin)
Landsat 5 (Band6)	607.76	1260.56
Landsat 7 (Band6)	666.09	1282.71
Landsat 8 (Band10)	774.89	1321.08
Landsat 8 (Band11)	480.89	1201.14

The LST is calculated by using thermal bands from LANDSAT-8 for Land Surface Temperature (LST) values in 10 &11 bands of LANDSAT-8 [18]. The Temperature values are in each band is taken from Radiance which was Digital number was converted to radiance. The LST image and mining cover image were compared with Boolean algebra functions to derive Mining Surface temperature of the mining existing within the basin as shown in the figure4.3. LANDSAT-8 methodology adopted was read from these images were in degree Kelvin (ºK) as 8 bit continuous data in WGS-84, 44N Zone projection such as AASTER satellite data [16]. LANDSAT-8 LST & MST degree Kelvin (ºK) data is converted into degree Celsius by using following equation [14]

$$°C = °K-273$$

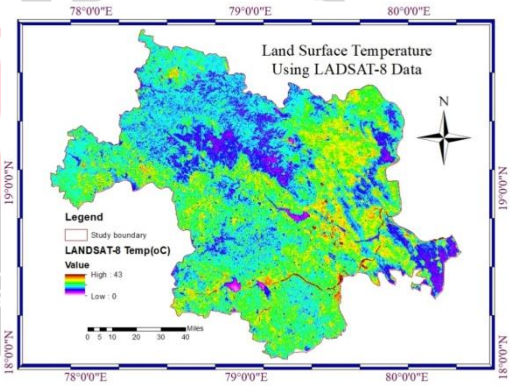

Fig4.3: Land surface Temperature (LST) from LANDSAT-8 data

AASTER Radiation and Land Surface Temperature

Proposed by the Ministry of Economy, Trade and Industry (METI) of Japan in collaboration with NASA, the Advanced Space borne Thermal Emission and Reflection Radiometer (ASTER) kinetic temperature and emissivity products [10, 16] offer a higher spatial resolution of 90 m, indeed data are potentially. Find out if AASTER data were available, search the AASTER archives at the EROS Data Center's Land Processes DAAC through the EDG [16]. All acquired and processed AASTER data were archived and distributed from here http://edcimswww.cr.usgs.gov/pub/imswelcome/. The AASTER Level-1B satellite data were offered in terms of scaled radiance. To convert from DN to radiance at the sensor, the unit conversion coefficients (defined as radiance per 1 DN) are used. Radiance (spectral radiance) is expressed in unit of W/(m^2*sr*µm). This product provides surface leaving radiance, in W m^{-2} sr^{-1} $µm^{-1}$, for the five ASTER TIR channels at 90 m spatial resolution. In addition, the down welling sky irradiance in W m^{-2} $µm^{1}$ for the two TIR bands ASTER TIR was provided. Atmospheric correction has been applied and the surface leaving radiance was valid for the clear sky portion of scenes. This radiance includes both surface emitted and surface reflected components. The surface radiance is only of known accuracy for cloud-free pixels. ASTER thermal bands constitute a valuable dataset for our research because both bands13 and 14 (Table 4.5) are similar to the single TIR channel of LANDSAT-8 (Table4.6) [18]. AASTER Data Satellite image-based Land Surface Temperature (LST) data were extracted using the Level 2B03 Product (surface kinetic temperature) from the thermal infrared (TIR) band of AASTER. The AASTER instrument, located onboard the Terra satellite, was composed of three sensors: SWIR (short wave infrared),

 DOI : 10.35291/2454-9150.2022.0489

VNIR (visible near infrared), and TIR (thermal infrared). It also has 14 spectrum bands to analyze radiance. Among them, the TIR generates products between channels 10 and 14 (8.15–11.65 μm) [16, 21]. The spatial resolution of the ASTER 2B03 product is 90m, and it is used to generate data for the Temperature Emissivity Separation (TES) algorithm used for determining the emissivity of land coverage values [24, 16]. This study collected AASTER satellite images on almost cloudless, sunny days at 8th February 2021. In particular, the acquisition times were at 01:10 pm UTC daytime. Surface temperatures were extracted after geometric corrections and coordinate transformations had been performed with reference by LANDSAT-8. The calculations were performed starting with the radiance at sensor as input. The radiance can be obtained from DN values of thermal bands of AASTER data as follows equation8 [16].

Radiance = (DN value – 1) x Unit conversion coefficient ---------8.

The maximum radiances depend on both the spectral bands and the gain settings as shown in Table 4.3. The Land Surface Temperature (LST) calculated using from gain, bias and digital pixel values of Thermal bands [14]. These were all values analyzed in Model maker algorithm.

Table: 4.3 Maximum Radiance Values for all AASTER Bands and all Gains used for Thermal bands

Band No.	Maximum radiance (W/(m ^{2} *sr*µm)			
	High gain	Normal Gain	Low Gain 1	Low gain 2
1	170.8	427	569	N/A
2	179.0	358	477	
3N	106.8	218	290	
3B	106.8	218	290	
4	27.5	55.0	73.3	73.3
5	8.8	17.6	23.4	103.5
6	7.9	15.8	21.0	98.7
7	7.55	15.1	20.1	83.8
8	5.27	10.55	14.06	62.0
9	4.02	8.04	10.72	67.0
10, 11 12, 13, 14	N/A		28.17, 27.75 26.97, 23.30, 21.38	N

***Table4.5.** AASTER thermal bands specifications.*

Band No	Wavelength(um)	Resolution(m)
10	8.125–8.475	90
11	8.475–8.825	90
12	8.925–9.275	90
13	10.25–10.95	90
14	10.95–11.65	90

The amount of radiance that an AASTER Thermal bands would be observe when viewing a source of a particular Temperature was calculated. The spectral radiance at each wavelength was computed using the Planck function [16]. This value is multiplied by the normalized spectral response function at that wavelength, and the results of this calculation are integrated over the range of wavelengths that have a sensor response. The above calculation was made for each of the two AASTER TIR bands at all Temperatures that the AASTER Thermal bands subsystem was designed to recorded in degrees Kelvin). The LST of the ground surface is obtained by multiplying with 0.02. The AASTER degree Kelvin (ºK) [16] data converted into degree Celsius by using following equation4.1in Model maker algorithm. The Land Surface Temperature derived from AASTER satellite data as shown in the figur4.5.

°C = ºK-273-------4.1

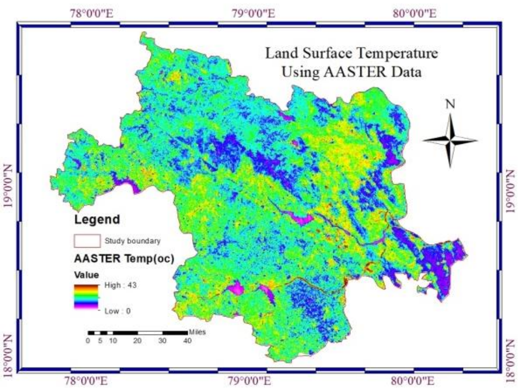

Fig4.5: Land surface temperature from AASTER satellite data

 DOI : 10.35291/2454-9150.2022.0489

International Journal for Research in Engineering Application & Management (IJREAM)
ISSN : 2454-9150 Vol-08, Issue-09, Dec 2022

IV. Analysis and Results

A statistical analysis was carried out between the LST derived from AASTER, LANDSAT-8 LST maps and air temperature measured in the field to determine the relationship and mutual comparison [14, 16, and 18]. The field temperature data measured at Mandal wise stations in Karimnagar & Adilabad at the Godavari basin have been used in this study as shown in the Fig.1. For comparison, to account for some locational errors, a 3x3 window is considered and LST values have been read for 9 pixels at the location corresponding to the field temperature station. The average of these 9 values has been considered to represent the location of temperature station. The AASTER derived LST is compared with Field measured air temperatures. Similarly the LANDSAT-8 LST map derived values have been compared with field measured air temperatures. Finally, the LST derived from AASTER and LANDSAT-8 is mutually compared comparison [14, 16, and18]. The details of comparison are explained in the following sections.

Fig.5.1: Location map of the AASTER and LANDSAT-8 Temperature With Field Temperature stations

Classification	Mandal	AASTER Temp	LANDSAT8 Temp	Field Temp	AASTER-LANDSAT8	AASTER-Field Temp	LANDSAT8-Field Temp
		C°	C°	C°	C°	C°	C°
Water Body Area	Narnoor	21	20	24	1	-3	-4
	Jainad	22	18	19	4	3	-1
	Bela	21	19	25	2	-4	-6
	Gadiguda	26	24	25	2	1	-1
	Bheempoor	30	25	26	5	4	-1
	Tamsi	22	17	18	5	4	-1
	Talamadugu	28	24	26	4	2	-2
	Adilabad Rural	30	27	27	3	3	0
	Adilabad Urban	28	26	32	2	-4	-6
	Mavala	29	30	27	-1	2	3
	Inderavelly	23	23	18	0	5	5
	Manakondur	18	22	16	-4	2	6
	Huzurabad	28	27	27	1	1	0
	Chandurthi	27	28	26	-1	1	2
	Gudihathnur	26	28	25	-2	1	3
Forest Area	Bazarhathnoor	29	30	28.6	-1	0.4	1.4
	Boath	27	31	28.7	-4	-1.7	2.3
	Neradigonda	29	30	29	-1	0	1
	Ichoda	29	28	31	1	-2	-3
	Kubeer	28	31	29	-3	-1	2
	Metpalle	28	31	27	-3	1	4
	Sirikonda	30	27	29.1	3	0.9	-2.1
	Utnur	22	23	21	-1	1	2
	Jainoor	28	30	29.2	-2	-1.2	0.8
	Sirpur_U	30	27	28	3	2	-1
	Lingapur	31	32	29.3	-1	1.7	2.7
	Tiryani	30	31	31	-1	-1	0
	Rebbana	30	31	29.4	-1	0.6	1.6
	Asifabad	38	37	39	1	-1	-2
	Kerameri	28	29	29.4	-1	-1.4	-0.4
	Wankdi	37	34	36	3	1	-2
	Kagaznagar	31	32	29.5	-1	1.5	2.5
	Sirpur_T	36	34	37	2	-1	-3
	Kouthala	28	32	29.7	-4	-1.7	2.3
	Chintalamanepally	29	28	28.1	1	0.9	-0.1
	Bejjur	27	28	29.7	-1	-2.7	-1.7
	Penchikalpet	27	29	30	-2	-3	-1
	Dahegaon	28	30	29.7	-2	-1.7	0.3
	Jannaram	29	31	31	-2	-2	0
	Dandepalle	28	30	29.8	-2	-1.8	0.2
Agric ulture	Luxettipet	29	31	29.8	-2	-0.8	1.2
	Hajipur	27	28	29.8	-1	-2.8	-1.8

Classification	Mandal	AASTER Temp	LANDSAT8 Temp	Field Temp	AASTER-LANDSAT8	AASTER-Field Temp	LANDSAT8-Field Temp
		C°	C°	C°	C°	C°	C°
Bair Soil Area	Sarangapur	31	33	30.4	-2	0.6	2.6
	Nirmal_Rural	32	34	35	-2	-3	-1
	Laxmanchanda	29	30	30.4	-1	-1.4	-0.4
	Mamda	28	29	30.4	-1	-2.4	-1.4
	Khanpur	29	34	31	-5	-2	3
	Kaddampeddur	31	33	30.5	-2	0.5	2.5
	Dastuarabad	34	31	35	3	-1	-4
	Ramadugu	33	30	30.5	3	2.5	-0.5
	Choppadandi	32	28	31	4	1	-3
	Karimnagar_Rural	34	27	30.6	7	3.4	-3.6
	Gannervaram	30	32	29	-2	1	3
	Karimnagar	29	32	31	-3	-2	1
	Thimmapur	28	31	30.7	-3	-2.7	0.3
	Chigurumamidi	29	32	33	-3	-4	-1
	Shankarapatnam	28	30	30.7	-2	-2.7	-0.7
Built-up Area	Veenavanka	28	32	31	-4	-3	1
	Jammikunta	32	28	30.7	4	1.3	-2.7
	Rudrangi	32	31	34	1	-2	-3
	Vemulawada_Rural	31	33	30.9	-2	0.1	2.1
	Vemulawada	34	32	29	2	5	3
	Mandamarri	32	29	31	3	1	-2
	Nirmal	32	33	33	-1	-1	0
	Kothapalle	32	29	31	3	1	-2
	V_Saidapur	27	32	29	-5	-2	3
	Boinpalle	30	32	31	-2	-1	1
	Sirsilla	32	34	35	-2	-3	-1
	Buggaram	30	31	31	-1	-1	0
	Gollapalle	34	33	36	1	-2	-3
	Julapalle	34	35	37	-1	-3	-2
	Konaraopeta	35	33	31.1	2	3.9	1.9
	Yellareddypeta	35	33	35	2	0	-2
	Mustabad	32	31	32	1	0	-1
	Ellanthakunta	30	28	34	2	-4	-6
	Mallapur	33	32	29	1	4	3
	Beerpur	30	30	28	0	2	2
	Dharmapuri	33	33	31.5	0	1.5	1.5
	Jagityal_Rural	29	31	32	-2	-3	-1
	Jagtial	30	31	33	-1	-3	-2
	Koratla	27	30	31.7	-3	-4.7	-1.7
	Kathlapur	31	30	29	1	2	1
minin g Area	Malial	32	29	27	3	5	2
	Lokeswaram	34	33	32	1	2	1

 DOI : 10.35291/2454-9150.2022.0489

ISSN : 2454-9150 Vol-08, Issue-09, Dec 2022

	Kasipet	28	30	28	-2	0	2		Soan	30	32	34	-2	-4	-2
	Tandur	29	31	29.8	-2	-0.8	1.2		Gambhiraopeta	34	34	32	0	2	2
	Bheemini	29	28	27	1	2	1		Ibrahimpatnam	30	31	33	-1	-3	-2
	Kannepalli	28	28	29.9	0	-1.9	-1.9		Pegadapalle	33	33	31	0	2	2
	Vemanpalle	28	27	28	1	0	-1		Ramagundam	39	41	38	-2	1	3
	Nennal	29	31	29.9	-2	-0.9	1.1		Ramagiri	39	40	36	-1	3	4
	Bellampalle	31	32	30	-1	1	2		Elgaid	34	33	35	1	-1	-2
	Mancherial	33	31	32	2	1	-1		Naspur	36	37	38	-1	-2	-1
	Jaipur	34	32	30	2	4	2		Bhainsa	31	29	31	2	0	-2
	Bhimaram	33	31	31	2	2	0		Ellandakunta	33	30	33	3	0	-3
	Chennur	28	32	30.1	-4	-2.1	1.9		Veernapalle	32	34	35	-2	-3	-1
	Kotapalle	29	32	28	-3	1	4		Medipalle	28	32	31	-4	-3	1
	Tanur	29	29	30.2	0	-1.2	-1.2		Sultanabad	35	36	37	-1	-2	-1
	Basar	28	27	27	1	1	0		Odela	36	32	33	4	3	-1
	Mudhole	29	28	30.2	1	-1.2	-2.2		Pembi	29	31	32	-2	-3	-1
	Kuntala	32	31	33	1	-1	-2		Gangadhara	34	33	36	1	-2	-3
	Narsapur_G	31	32	30.3	-1	0.7	1.7		Thangallapalle	31	31	34	0	-3	-3
	Dilawarpur	32	36	33	-4	-1	3		Sarangapur	32	32	35	0	-3	-3

Comparison of Land Surface Temperature Derived from AASTER, LANDSAT-8 and Field Air Temperature

The LST values derived from AASTER data at different locations corresponding to the field temperature gauge stations have been compared as shown in Table5.1 the maximum and minimum air temperature recorded in field is considered for comparison. The AASTER satellite overpass at equator is at about 10:30 Am Eastern Standard Time(EST). Terra files Sun synchronous polar orbit crossing the equator at the time. The satellite overpass time of LANDSAT-8 is at about 10:00Am. +/-15minutes (Mean local time) in their respective orbit at equator. The Landsat-8 satellite each acquire data in accordance with their respective Long Term Acquisition Plan(LTAP) using parameters such as seasonally, land definition, historical cloud cover, gain setting and sun angles. Travelling on descending (day time) node from north to south , the satellite cross the equator on each pass at a time that provide the maximum illumination with minimum water vapor(haze and cloud built-up).

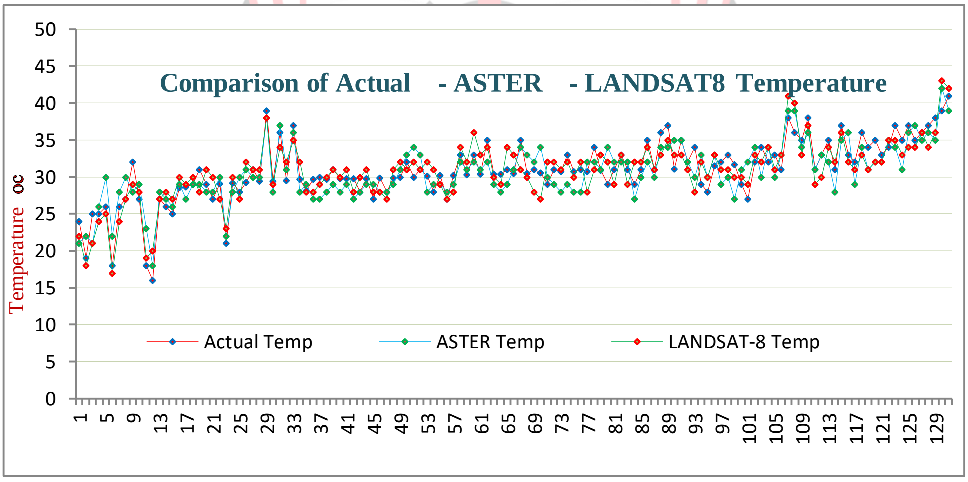

Fig.5.1: LST Comparison of LST derived from AASTER, LANDSAT-8 and field air temperatures

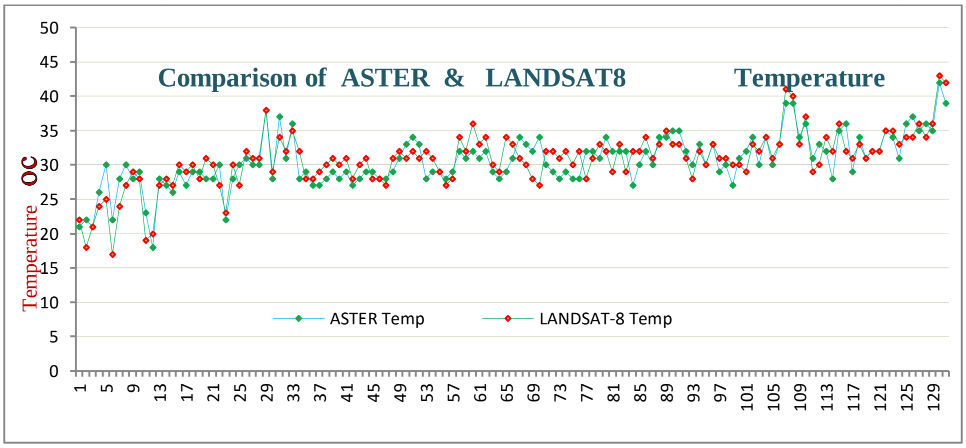

Fig.5.2: LST Comparison of LST derived from AATER and LANDSAT-8

 DOI : 10.35291/2454-9150.2022.0489

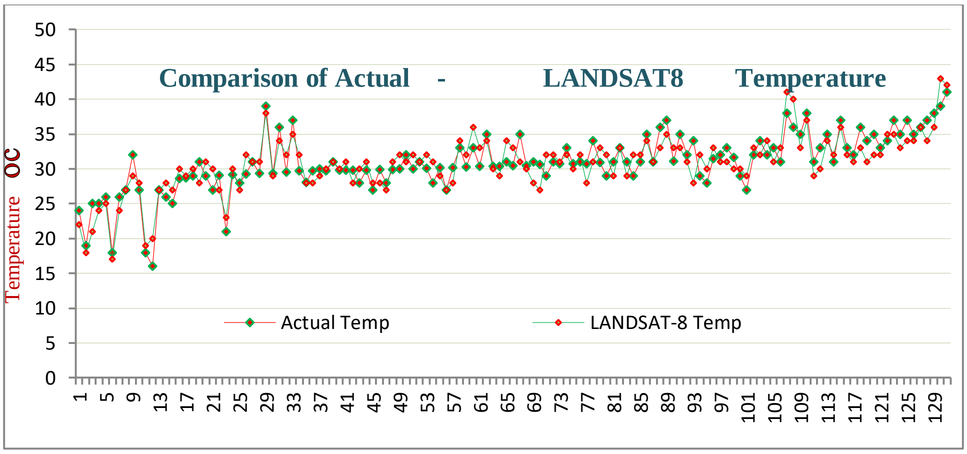

Fig.5.3: LST Comparison of LST derived from Field air temperature and LANDSAT-8

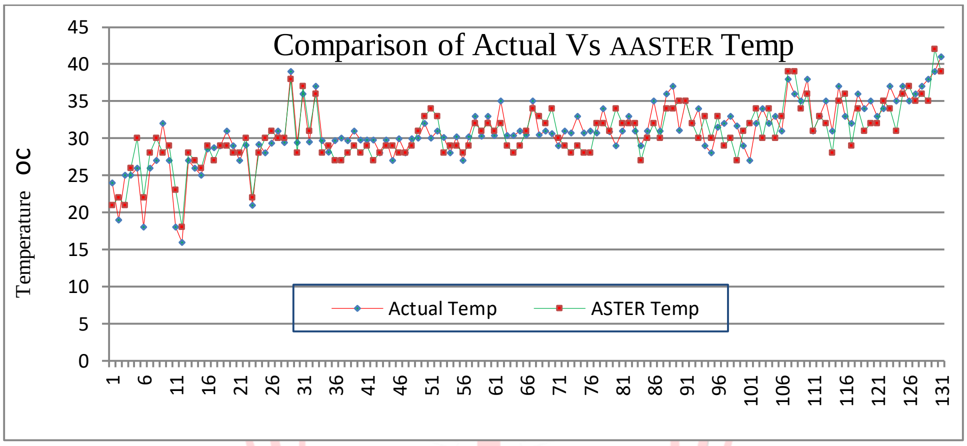

Fig .5.4: LST Comparison of LST derived from AASTER and field air temperatures

The LST corresponds to the surface whereas the field measured air temperature corresponds to a point in air at about 1m. Above the ground the deviation between the LST obtained from AASTER data and field air temperature is generally within +/- 3º. The deviation between the LST obtained from LANDSAT-8 data and field air temperature is generally within +/- 4º. The deviation between LST derived from AASTER data and that of LANDSAT-8 data is generally within +/- 4º. In view of the above cited reasons the deviations may still be acceptable.

1.2. Statistical Analysis and Verification for Temperature

Correlation analysis has been made between the LST derived from AASTER data and field air temperature and calculated the bias and standard deviation of the regression. The field air temperature is considered as dependent variable and AASTER LST is considered as independent variable. The values of Constant(c), X Coefficient, R^2 and Std Err of Coefficient are tabulated in Table 5.2. [14]

$$T_c = b0.746 \times T_n + 7.35358$$

Where T_n –AASTER Temperature.

T_c – Field temperature.

Table 5.2: Regression Output values using AASTER & field temperature

Regression Statistics						
Observations	Standard Error	Adjusted R Square	R Square	Multiple R		Upper 95.0%
59	1.7252174	0.7852116	0.7994321	0.871454		10.565959
						0.8583696
	df	SS	MS	F	Significance F	Lower 95.0%
Regression	1	535.56696	535.56696	179.93933	2.79E-19	4.1411106
Residual	57	169.65338	2.9763751			0.6353821
Total	58	705.22034				

 DOI : 10.35291/2454-9150.2022.0489

	Coefficients	Standard Error	t Stat	P-value	Lower 95%	Upper 95%
Intercept	7.3535348	1.6042346	4.5838277	2.54E-05	4.1411106	10.565959
24	0.7468759	0.0556782	13.414147	2.79E-19	0.6353821	0.8583696

The above regression equation has been verified by estimating the air temperature at some selected Mandal station. The LST value at the locations has been derived from AASTER data and air temperature has been computed. The computed air temperature is then compared with actual measured air temperature at the locations as shown in Table 5.3.

Table 5.3: Actual Field air Temperature and computing Values of AASTER Temperature

Mandal	Actual Temp	Computed Temp from AASTER Temp	Deviation	Mandal	Actual Temp	Computed Temp from AASTER Temp	Deviation
	C°	C°	C°		C°	C°	C°
Rudrangi	34	30.9	3.1	Ibrahimpatnam	33	31	2
Vemulawada_Rural	30.9	29	1.9	Pegadapalle	31	38	-7
Vemulawada	29	31	-2	Ramagundam	38	36	2
Mandamarri	31	33	-2	Ramagiri	36	35	1
Nirmal	33	31	2	Elgaid	35	38	-3
Kothapalle	31	29	2	Naspur	38	31	7
V_Saidapur	29	31	-2	Bhainsa	31	33	-2
Boinpalle	31	35	-4	Ellandakunta	33	35	-2
Sirsilla	35	31	4	Veernapalle	35	31	4
Buggaram	31	36	-5	Medipalle	31	37	-6
Gollapalle	36	37	-1	Sultanabad	37	33	4
Julapalle	37	31.1	5.9	Odela	33	32	1
Konaraopeta	31.1	35	-3.9	Pembi	32	36	-4
Yellareddypeta	35	32	3	Gangadhara	36	34	2
Mustabad	32	34	-2	Thangallapalle	34	35	-1
Ellanthakunta	34	29	5	Sarangapur	35	33	2
Mallapur	29	28	1	Kodimial	33	34	-1
Beerpur	28	31.5	-3.5	Velgatoor	34	37	-3
Dharmapuri	31.5	32	-0.5	Palakurthy	37	35	2
Jagityal_Rural	32	33	-1	Raikal	35	37	-2
Jagtial	33	31.7	1.3	Antargoan	37	35	2
Koratla	31.7	29	2.7	Srirampur	35	36	-1
Kathlapur	29	27	2	Dharmaram	36	37	-1
Malial	27	32	-5	Mutharam_Manthani	37	38	-1
Lokeswaram	32	34	-2	Kamanpur	38	39	-1
Soan	34	32	2	Peddapalle	39	41	-2
Gambhiraopeta	32	33	-1	Manthani	41	40	1

The comparison of actual air temperature with computed air temperature shows that the deviation is within +/- 3° as shown in the figure5.5.5. In view of the reasons for possible deviation as explained in earlier section, the results are acceptable and can be employed. However, for more precise applications, the work can be done with some more stations and for more number of dates so that the computed equation can be operationally used for Mining area modeling purpose. Constant(c), X Coefficient, R Square and Std Err of Coefficient values computed in the regression analysis with input values of LANDSAT-8 data Temperature and actual temperature of some selected Mandal shown in Table 5.4.

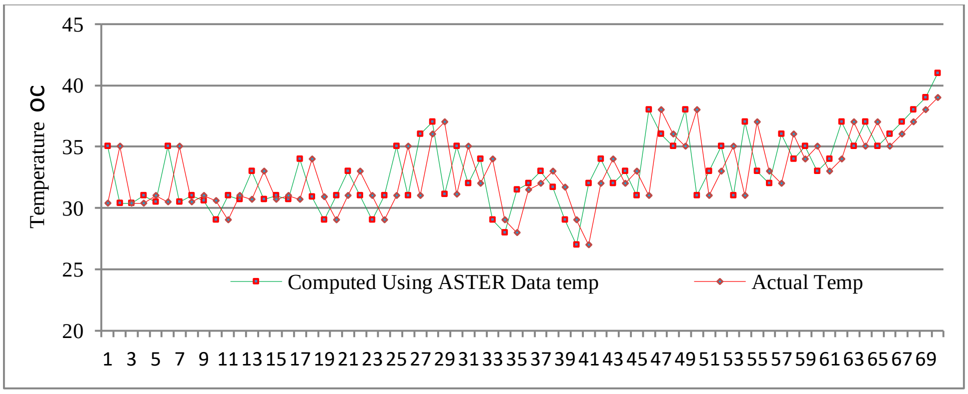

Fig 5.5: comparison in between actual and computed using LANDSAT-8 Temperature

 DOI : 10.35291/2454-9150.2022.0489

ISSN : 2454-9150 Vol-08, Issue-09, Dec 2022

Table 5.4: Regression Output values

Regression Statistics					
Observations	Standard Error	Adjusted R Square	R Square	Multiple R	Upper 95.0%
59	1.7252174	0.7552116	0.7594321	0.871454	10.565959
					0.8583696
	df	SS	MS	F	Significance F
Regression	1	535.56696	535.56696	179.93933	2.79E-19
Residual	57	169.65338	2.9763751		Upper 95%
Total	58	705.22034			10.565959
	Coefficients	Standard Error	t Stat	P-value	Lower 95%
Intercept	7.2535348	1.6042346	4.5838277	2.54E-05	4.1411106
24	0.7568759	0.0556782	13.414147	2.79E-19	0.6353821

$$T_c = 0.75668759 \times T_n + 7.25353488$$

Where T_n –LANDSAT-8 Temperature. T_c – Field temperature. The above regression equation values of constant, X coefficient values are used in Godavari Basin station to calculate values of computing field temperature. Result of computing LANDSAT-8 temperature values as shown in the table 5.5.

Table 5.5: Actual Field air Temperature and computing Values of AASTER Temperature

Mandal	Actual Temp	Computed Temp from LANDSAT-8	Deviation		Mandal	Actual Temp	Computed Temp from LANDSAT-8	Deviation
	C°	C°	C°			C°	C°	C°
Rudrangi	34	31	3		Pegadapalle	31	33	-2
Vemulawada_Rural	30.9	33	-2.1		Ramagundam	38	40	-2
Vemulawada	29	32	-3		Ramagiri	36	39	-3
Mandamarri	31	29	2		Elgaid	35	33	2
Nirmal	33	33	0		Naspur	38	36	2
Kothapalle	31	29	2		Bhainsa	31	29	2
V_Saidapur	29	32	-3		Ellandakunta	33	30	3
Boinpalle	31	32	-1		Veernapalle	35	34	1
Sirsilla	35	34	1		Medipalle	31	32	-1
Buggaram	31	31	0		Sultanabad	37	35	2
Gollapalle	36	33	3		Odela	33	32	1
Julapalle	37	35	2		Pembi	32	31	1
Konaraopeta	31.1	33	-1.9		Gangadhara	36	33	3
Yellareddypeta	35	33	2		Thangallapalle	34	31	3
Mustabad	32	31	1		Sarangapur	35	32	3
Ellanthakunta	34	28	6		Kodimial	33	32	1
Mallapur	29	32	-3		Velgatoor	34	35	-1
Beerpur	28	30	-2		Palakurthy	37	35	2
Dharmapuri	31.5	33	-1.5		Raikal	35	33	2
Jagityal_Rural	32	31	1		Antargoan	37	34	3
Jagtial	33	31	2		Srirampur	35	34	1
Koratla	31.7	30	1.7		Dharmaram	36	35	1
Kathlapur	29	30	-1		Mutharam_Manthani	37	34	3
Malial	27	29	-2		Kamanpur	38	35	3
Lokeswaram	32	33	-1		Peddapalle	39	42	-3
Soan	34	32	2		Manthani	41	41	0
Gambhiraopeta	32	34	-2		Pegadapalle	31	33	-2
Ibrahimpatnam	33	31	2		Ramagundam	38	40	-2

 DOI : 10.35291/2454-9150.2022.0489

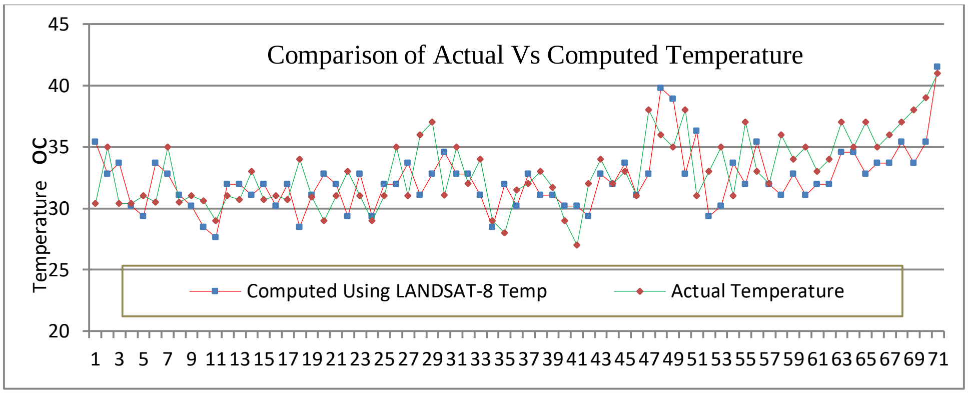

Fig.5.6: comparison in between actual and computed using LANDSAT-8 temperature

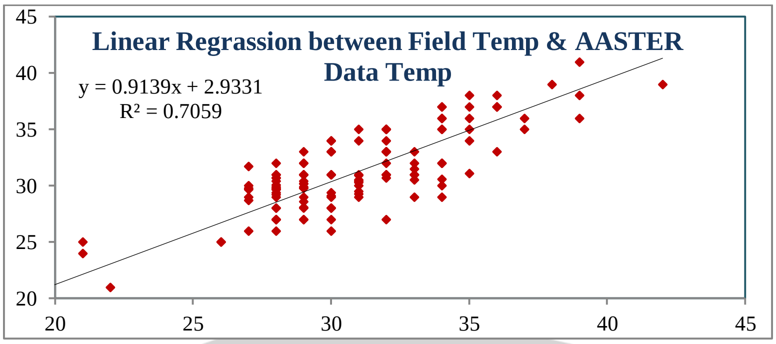

Figure 5.7: Analysis results for pixel-based surface Temperature collected by AASTER images Temperature and field air Temperature.

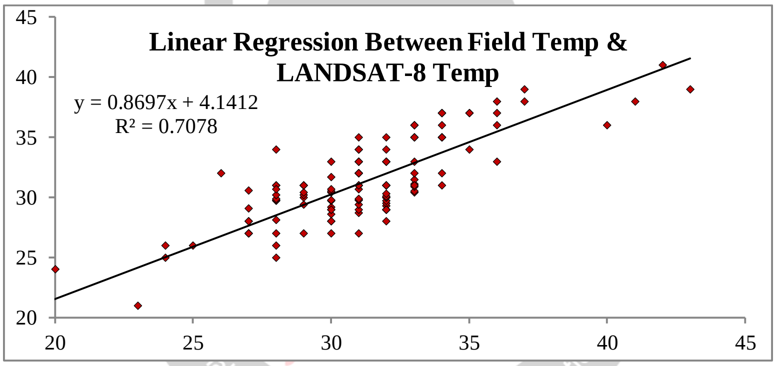

Figure 5.8: Analysis results for pixel-based surface Temperature collected by LANDSAT-8 images Temperature and field air Temperature.

Results were compared with ground temperature data, resulting in high correlation factors, indicating that the estimated surface temperature is a good match to observed value a shown in the figure5.6. Thus it may be concluded that, the LST estimated from satellite data can be used in Mining modeling as an alternative in absence of ground measured temperature data.

V. CONCLUSION

In Mining studies, energy input to the Mining Surface Temperature is an important component. Generally, ground measured temperature used as an alternative indicator of energy input. In rugged terrain such as the meteorological stations collecting ground temperature data are sparsely located and the observations, being point data, are not representative of the whole area. In addition, the Land Surface Temperature (LST) is measured manually and hence it is susceptible to errors. In such conditions, LST maps prepared from satellite images are an attractive alternative. This approach can also be used for estimation of LST. The AASTER images and LANDSAT-8 LST maps are economical and suitable. In addition, these datasets are available for near real time, providing a further advantage. There is research potential for the use of LST data in Mining computations. The Land Surface Temperature (LST) computed from AASTER and LANDSAT-8 satellite data using Thermal Bands are useful for Godavari basin in absence of well distributed field measurements of air temperatures. The LST explains the spatial variability over the entire basin whereas the field air temperature measurements at a few stations indicate local weather conditions. In addition, since the field stations are generally located at lower altitudes, generally above 5m in Godavari basin, do not explain the variability in the vertical plane as the Mining land is predominantly from approximately elevations from 10 to 20m above earth. The LST derived from AASTER and LANDSAT-8 data are in coherence. The LST derived from satellite data is comparable with

 DOI : 10.35291/2454-9150.2022.0489

field measured air temperatures. The estimated LST values and Field air temperature have a general difference of about 4º. However, the factors such as, time of satellite overpass, possible inaccuracies in exact locations of field stations and coarse spatial resolution of satellite data are responsible for some deviations in the actual measured and estimated temperatures. This experiment with larger data set and some more field stations can improve the accuracy of estimation.

VI. REFERENCE

[1] Prakash, A. Thermal remote sensing: Concepts, issues and applications. In Proceedings of the International Archives of Photogrammetry and Remote Sensing, Amsterdam, the Netherlands, 16–22 July 2002; Volume 23, pp. 239–243.

[2] Kahle, A.B. Surface thermal properties. In Remote Sensing in Geology; Siegal, B.S., Gillespie, A.R., Eds.; John Wiley & Sons, Inc.: New York, NY, USA, 1980; pp. 257–273. ISBN 0471790524.

[3] Sabins, F.F. Remote Sensing: Principles and Interpretation, 3rd ed.;W. H. Freeman: New York, NY, USA, 1996;ISBN 0716724421. Wan, Z.; Dozier, J. A generalized split-window algorithm for retrieving land-surface temperature from space. IEEE Trans. Geosci. Remote Sens. 1996, 34, 892–905.

[4] Meng, X.; Cheng, J.; Liang, S. Estimating land surface temperature from Feng Yun-3C/MERSI data using a new land surface emissivity scheme. Remote Sens. 2017, 9, 1247.

[5] Dozier, J.; Warren, S.G. E_ect of viewing angle on the infrared brightness temperature of mining. Water Resour. Res. 1982, 18, 1424–1434.

[6] Schlapfer, D.; Borel, C.C.; Keller, J.; Itten, K.I. Atmospheric Precorrected Differential Absorption Technique to Retrieve ColumnarWater Vapor. Remote Sens. Environ. 1998, 65, 353–366.

[7] Obata, K.; Tsuchida, S.; Yamamoto, H.; Thome, K. Cross-calibration between ASTER and MODIS visible to near-infrared bands for improvement of ASTER radiometric calibration. Sensors 2017, 17, 1793.

[8] Ma, Y.; Zhang, Y.; Mei, X.; Dai, X.; Ma, J. Multifeature-Based Discriminative Label Consistent K-SVD for Hyperspectral Image Classification. IEEE J. Sel. Top. Appl. Earth Obs. Remote Sens. 2019, 12, 4995–5008.

[9] hao, Z.; Zhang, L. Sparse dimensionality reduction of hyperspectral image based on semi-supervised local Fisher discriminant analysis. Int. J. Appl. Earth Obs. Geoinf. 2014, 31, 122–129.

[10] Indian Coal and Lignite Resource- 2017. Geological Survey of India. https://gsi.gov. in/cs/groups/public/documents/document/b3zp/mtyx/~edisp/dcport1gsigovi161863pdf (accessed 12.11.17)

[11] CWC, 2013. http://www.indiawaterportal.org/author/cetral-water-commossion- CWC. (accessed 08.01.14)

[12] Provisional Coal Statistics, 2015-16. http://www.coalcontroller.gov.in writereaddata/files/Provisional%20Coal%20Statistics%202015-16 pdf (accessed 11.03.17).

[13] Provisional Production and Dispatches Performance of SCCL, 2017. https:// scclmines.com /scclnew/performance_production.asp. (accessed 21.08.17).

[14] NagarajuThummala, E. Sivasanker, E. Srinivas, B.Sridhar. 2018 'Estimation of Surface Temperature Using Satellite Data in Sutlej Basin' International Journal of Engineering, Science and Mathematics, Vol.7Issue 3, March2018, ISSN: 2320-0294 Impact Factor: 6.765 Journal Homepage: http://www.ijesm.co.in. Email: ijesmj@gmail.com. U.S.A., Open J-Gage as well as in Cabell's Directories of Publishing Opportunities, U.S.A.

[15] Areendran, G., Rao, P., Raj, K., Majumdar, S., Puri, K., 2013. Land use/land cover change dynamics analysis in mining areas of Singrauli district in Madhya Pradesh India. Trop. Ecol. 54 (2), 239–250.

[16] Ndossi, M.; Avdan, U. Inversion of land surface temperature (LST) using terra ASTER data: A comparison of three algorithms. Remote Sens. 2016, 8, 993.

[17] Open Data Telangana' (ODT) from the website browser http://data.telangana.govt.in/dataset/telangana- temperature-data-2022/resource in.

[18] Sekertekin, A. Validation of physical radiative transfer equation-based land surface temperature using Landsat 8 satellite imagery and SURFRAD in-situ measurements. J. Atmos. Solar Terr. Phys. 2019, 196, 105161.

[19] Ndossi, M.; Avdan, U. Inversion of land surface temperature (LST) using terra ASTER data: A comparison of three algorithms. Remote Sens. 2016, 8, 993.

[20] Choudhury, Nizam U Ahmed, Sherwood B Idso, (1994) 'Relation between evaporation coefiecent and vegetation indexstudeis by simulation. Elsever publisher, Remote sensing of environment publication. https://doi.org/10.1016/0034-4257(94)90090-6.

[21] Cook, M. Atmospheric Compensation for a Landsat Land Surface Temperature Product. Ph.D. Thesis, Rochester Institute of Technology, Rochester, NY, USA, 2014.

[22] Dozier, J.; Warren, S.G. E_ect of viewing angle on the infrared brightness temperature of mining. Water Resour. Res. 1982, 18, 1424–1434.

[23] Wan, Z.; Li, Z.-L. Radiance-based validation of the V5 MODIS land-surface temperature product. Int. J. Remote Sens. 2008, 29, 5373–5395.

[24] Sobrino, J.A.; Raissouni, N.; Li, Z. A comparative study of land surface emissivity retrieval from NOAA data. Remote Sens. Environ. 2001, 75, 256–266.

 DOI : 10.35291/2454-9150.2022.0489